BLM injection. Serum IL-6 levels were undetectable by enzyme-linked immunosorbent assay in all PBS-treated mice, and in 3 of 11 C57BL/6 mice treated with BLM. However, IL-6 was detectable, thus elevated, in 8 of 11 BLM-treated mice (Figure 1A), with a mean of 11.9 ± 5.24 pg/mL (n = 8). IL-6 mRNA expression showed a trend toward increased levels in the skin of mice treated with BLM that was not statistically significant (Figure 1B), and was significantly elevated ($P < 0.05$) in the cutaneous draining LNs of BLM-treated mice relative to PBS-treated mice (Figure 1C). These results are consistent with a role for IL-6 in the pathogenesis of scleroderma in the BLM-induced mouse model.

MR16-1 Prevents BLM-Induced Dermal Sclerosis

We next investigated whether MR16-1, a rat anti-mouse IL-6 receptor monoclonal Ab, could ameliorate the dermal thickening and skin hardening symptoms observed in BLM-treated mice. Figure 2A shows the administration schedule of preventive intervention. Dermal thickness was significantly increased at the BLM injection site of control Ab–treated mice, but nearly normal at the PBS injection site of control Ab–, or MR16-1–treated mice. Importantly, BLM-induced dermal thickening was significantly attenuated by prophylactic administration of MR16-1 (Figure 2, B and C, Table 1).

Skin hardness in the BLM-injected group that was given MR16-1 was also significantly reduced compared to the BLM-injected group that was given the control Ab. The ameliorating effect of MR16-1 on skin hardness was relatively strong compared with the effect on dermal thickness (Figure 2, B and D, Table 1).

To further examine the effects of MR16-1 treatment, the numbers of α-SMA–positive fibroblasts (termed myofibroblasts) (Figure 2, E and F, Table 1) and mast cells (Figure 2, G and H, Table 1), both key players in sclerosis of skin lesions, were evaluated. The numbers of myofibroblasts and mast cells were significantly increased in BLM-injected mice treated with control Ab relative to PBS-injected mice treated with control Ab. In BLM-injected mice treated with MR16-1, the numbers of myofibroblasts and mast cells were decreased significantly compared to the control value (BLM-injected mice treated with control Ab) (Figure 2, E to H, Table 1). These results suggest that treatment with MR16-1 might be effective during the fibrosing phase of scleroderma.

MR16-1 Improves BLM-Induced Dermal Sclerosis

Figure 3A shows the administration schedule of treatment intervention. As expected, the dermal thickness and skin hardness induced by BLM were diminished by therapeutic administration of MR16-1 compared with control Ab (Figure 3, B to D). The numbers of myofibroblasts and mast cells in lesional skin were also decreased by administration of MR16-1 compared with control Ab (Figure 3, E and F). Table 2 summarizes the data from two treatment intervention experiments. These results indicate that IL-6 may contribute to the pathogenesis of BLM-induced scleroderma and that blockade of IL-6 receptor may be a novel treatment of scleroderma.

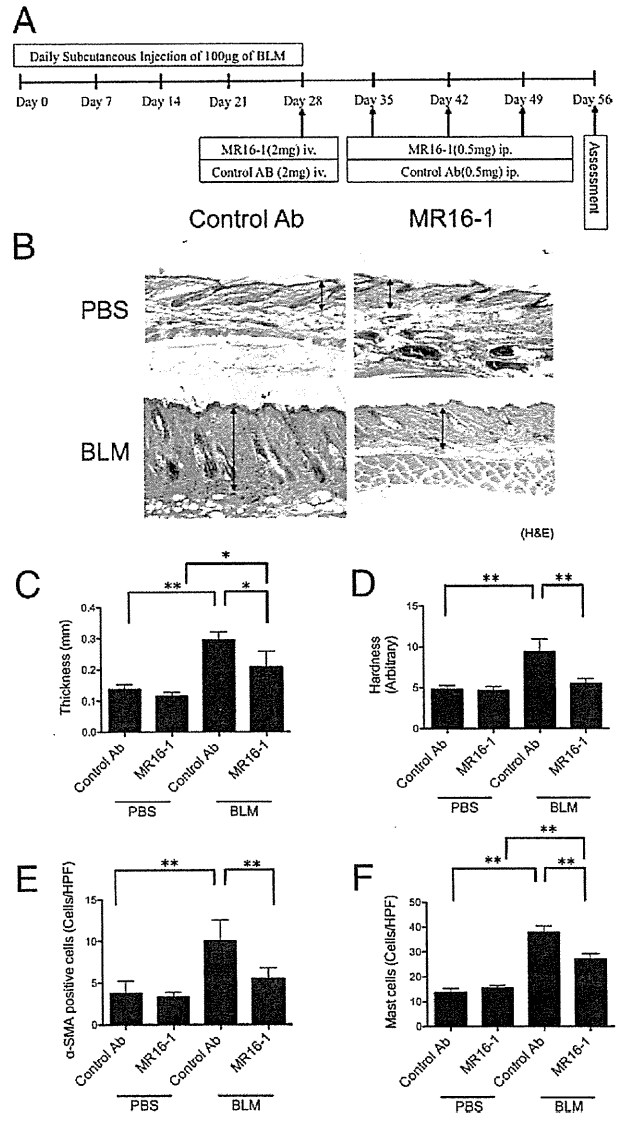

Figure 3. Effect of MR16-1 on BLM-induced dermal sclerosis in a treatment model. **A:** Experimental protocol for treatment of BLM-induced dermal sclerosis by administration of MR16-1 or control Ab to either PBS- or BLM-treated mice (n = 3~4 for each group). The effect of Ab therapy was assessed on day 56. **B:** H&E staining of specimens derived from PBS- or BLM-injected mice treated with MR16-1 or control Ab (original magnification, ×40), and measurements of dermal thickness (**C**) (the measurement region of dermal thickness was indicated with the length of each **two-headed arrow** in **B**) and skin hardness (**D**). The number of α-SMA–positive fibroblasts (**E**) and mast cells (**F**) per HPF (×400) were determined by observation of 10 random grids. The value graphed is the average of the observation of 10 grids for each of the four mice in the group. **C** to **F:** Bars represent mean ± SD. $^{*}P < 0.05$, $^{**}P < 0.01$, one-way analysis of variance and Bonferroni post hoc multiple comparison. Data presented are from the first of two independent experiments with similar results. See Table 2 for data from both experiments.

IL-6 Directly Modulates α-SMA Expression in Dermal Fibroblasts in Vitro

We next focused on whether dermal fibroblasts are a target of IL-6. Nontreated primary dermal fibroblasts from wild-type mice already express α-SMA, and stimulation

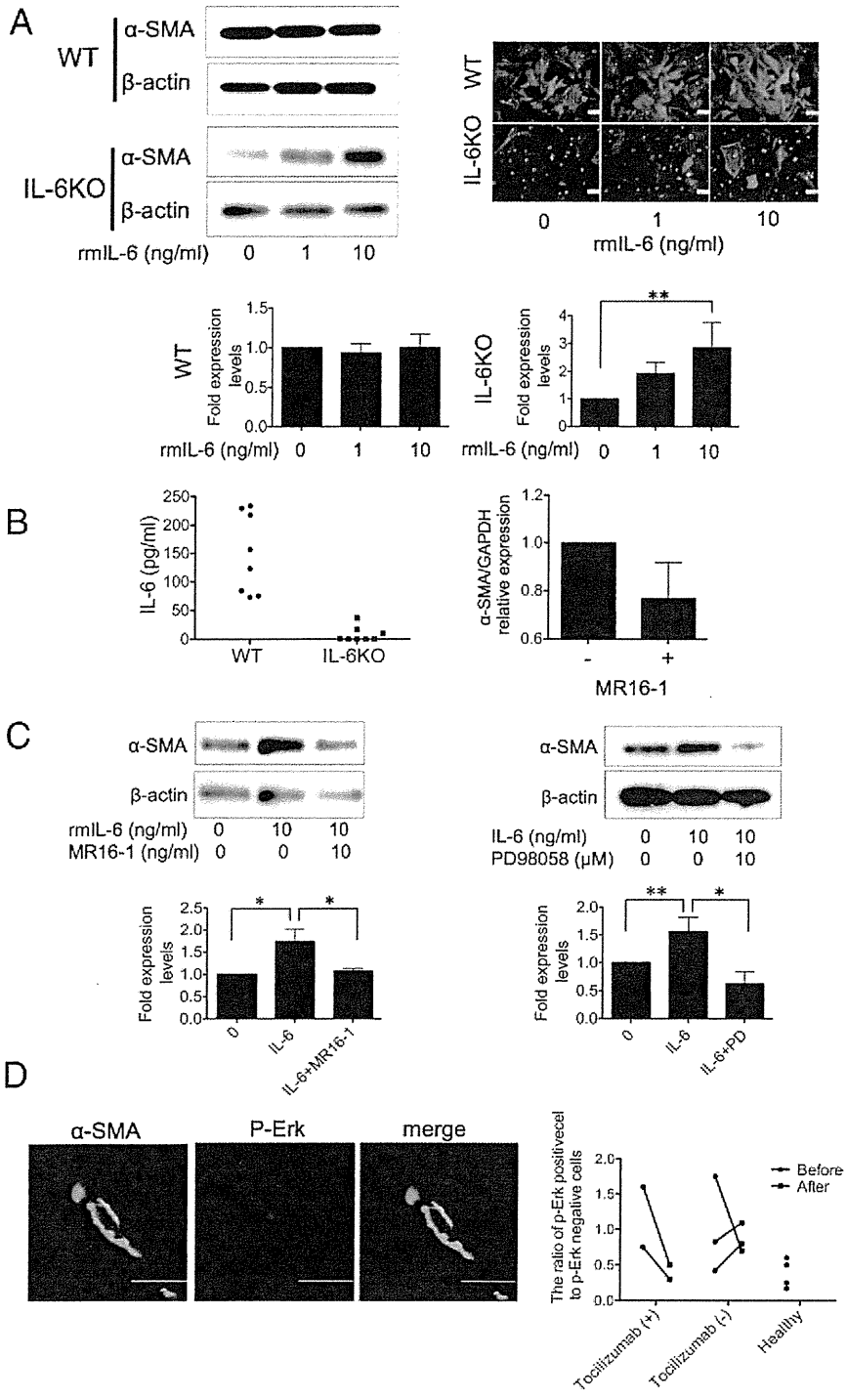

Figure 4. IL-6 induces α-SMA protein expression in cultured *Il-6*KO fibroblasts. **A:** α-SMA expression following recombinant mouse Il-6 (rmIL-6) stimulation was determined by immunofluorescent staining and Western blot analysis. α-SMA and nucleus were show in green and blue, respectively. Scale bar = 100 μm. β-Actin expression was used to determine fold changes in expression by densitometry. Cultured dermal fibroblasts from wild-type (WT) and *Il-6*KO mice were treated with 0, 1, and 10 ng/mL rmIL-6 for 24 hours. These experiments were repeated three times, and the results of densitometric analyses are presented as the fold change (mean ± SD) compared with control. $^{**}P < 0.01$, one-way analysis of variance and Bonferroni post hoc multiple comparisons. **B:** *Il-6* levels in supernatants of cultured dermal fibroblasts from WT and *Il-6*KO mice (**left**) after 24 hours. MR16-1 treatment decreased α-SMA mRNA expression in cultured primary WT dermal fibroblasts (**right**). **C:** MR16-1 and ERK inhibitor, PD98058, attenuated rmIL-6–induced α-SMA protein expression in cultured *Il-6*KO fibroblasts. β-Actin expression was used to determine fold changes in expression by densitometry. These experiments were performed three times, and the results of densitometric analyses are presented as the fold change (mean ± SD) compared with control. $^{**}P < 0.01$, $^{*}P < 0.05$, one-way analysis of variance and Bonferroni post hoc multiple comparisons. **D:** Immunofluorescent staining for phosphorylated ERK (p-ERK, red) and α-SMA (green) in lesional skin derived from two tocilizumab-treated patients with scleroderma. A representative image of p-ERK$^+$, α-SMA$^+$ fibroblasts (original magnification, ×1200) is shown. The number of p-ERK–positive α-SMA–positive fibroblasts per HPF (×400) was determined by observation of 10 random grids. Scale bar = 50 μm. The ratio of p-ERK–positive fibroblasts was calculated as follows: the number of p-ERK$^+$, α-SMA$^+$ fibroblasts/the number of p-ERK$^-$, α-SMA$^+$ fibroblasts.

with exogenous recombinant mouse IL-6 (rmIL-6) did not alter α-SMA expression (Figure 4A). Further, highly expressed levels of endogenous IL-6 from nontreated cultured primary wild-type dermal fibroblasts and decreased levels of α-SMA mRNA expression after MR16 treatment indicated that hyporesponsiveness of cultured primary wild-type dermal fibroblasts to exogenous IL-6 was presumably due to the autocrine regulation of α-SMA by IL-6 (Figure 4B). Thus, we switched to primary *Il-6*KO mouse–derived fibroblasts and evaluated α-SMA expression using immunofluorescent staining and Western blot analysis. Low-level expression was observed in nontreated *Il-6*KO dermal fibroblasts, but stimulation with 1 or 10 ng/mL of rmIL-6 induced α-SMA expression in a dose-dependent manner (Figure 4A). α-SMA induction by rmIL-6 was inhibited by 10 ng/mL MR16-1 and also by the ERK1/2 inhibitor PD98059 (Figure 4C).

These results led us to examine whether the positive effects of clinical treatment with tocilizumab might correlate with reduced numbers of ERK-activated α-SMA–pos-

itive dermal fibroblasts in lesional skin of scleroderma patients. The number of Erk-activated α-SMA–positive cells in lesional skin in scleroderma patients treated with tocilizumab for 6 months was reduced to a similar level as in healthy skin, whereas the number in scleroderma patients treated with 10 mg/day of prednisolone for 6 months without tocilizumab was diminished in one patient and increased in two patients (Figure 4D).

Attenuated BLM-Induces Dermal Sclerosis in Il-6KO Mice

To investigate the role of IL-6 in BLM-induced dermal sclerosis, *Il-6*KO mice received subcutaneous injection of BLM or PBS for 4 weeks, and histological and physical examination of the lesional skin was performed (Figure 5A, Table 3). We found that BLM-induced dermal sclerosis in *Il-6*KO mice was attenuated compared with that in wild-type mice. Lack of visible changes in the skin between PBS-treated *Il-6*KO mice and PBS-treated wild-type mice indicated that IL-6 might not be involved in dermal homeostasis (Figure 5A). After 4 weeks of BLM treatment, dermal thickness and skin hardness in *Il-6*KO mice were significantly attenuated compared to wild-type mice (Figure 5A). The numbers of α-SMA–positive cells and mast cells in BLM-treated *Il-6*KO mice were significantly reduced compared to BLM-treated wild-type mice (Figure 5B). Table 3 summarizes the data from two experiments. These results indicate that IL-6 is likely to play an important role in promoting the fibrogenic responses elicited by BLM treatment.

Enlarged Draining LNs Are Reduced in Size by a Block of IL-6 in the Mouse Model and in a Patient with Scleroderma

We found that cutaneous draining LNs were visibly enlarged by BLM treatment in the scleroderma model mice, but not by PBS treatment (Figure 6A, Table 4). The total LN cell count per LN in control Ab–treated BLM-injected mice was significantly increased compared with control Ab–treated PBS-injected mice, and decreased by administration of MR16-1 to BLM-injected mice. Although it was only from a single experiment with a small number of mice, the weight per LN also showed similar findings to the results of the total LN cell count per LN. However, no histological differences were observed between LNs from BLM- and PBS-injected control Ab–treated mice (Figure 6A). Detailed cell fractionation analysis (using cell-surface antigens CD4, CD8, B220, CD11c, F4/80, and PDCA1) of cells isolated from the draining LNs revealed that the ratio of $PDCA1^{+}CD11c^{+}$ double-positive cells [plasmacytoid dendritic cells (pDCs)] was significantly increased in the draining LNs of prophylactically MR16-1–treated model mice (Figure 6B). Further, draining LNs were not grossly enlarged in BLM-treated *Il-6*KO mice (Figure 6C, Table 4), consistent with weight and total cell count per LN measurements in the normal range (Figure 6C).

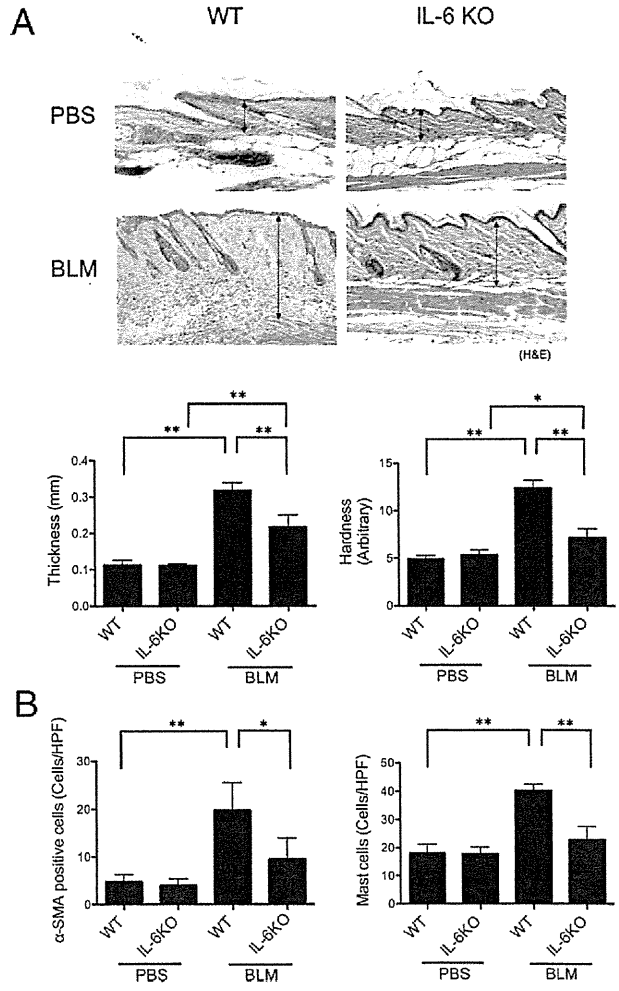

Figure 5. Attenuated BLM-induced dermal sclerosis in *Il-6*KO mice. **A:** H&E staining of skin specimen derived from PBS- and BLM-treated wild-type (WT) and *Il-6*KO mice (original magnification × 40), and measurements of dermal thickness (**lower left panel**) and skin hardness (**lower right panel**). The length of the **two-headed arrows** indicates the measurement region of dermal thickness. **B:** The number of α-SMA–positive fibroblasts (**left panel**) and mast cells (**right panel**) per HPF (×400) was determined by observation of 10 random grids. **A** and **B:** Bars represent mean ± SD ($n = 4$ for each group). $^{*}P < 0.05$, $^{**}P < 0.01$, one-way analysis of variance and Bonferroni post hoc multiple comparison. Data presented are from the first of two independent experiments that yielded similar results, and Table 3 presents data from both experiments.

We then examined whether LNs were enlarged in a patient with scleroderma, and found swelling of axillary LNs on computed tomography scan (Figure 6D), which was not detected after the administration of tocilizumab (Figure 6D).

Discussion

Our study demonstrates the critical role of IL-6 in dermal sclerosis. Blockade of IL-6 receptor with MR16-1 in the BLM-treated mice alleviates dermal sclerosis. This report also addresses outstanding problems in scleroderma pathogenesis, including the target of IL-6.

The source(s) of the elevated IL-6 in the sera of patients with scleroderma are still unclear. Several lines of

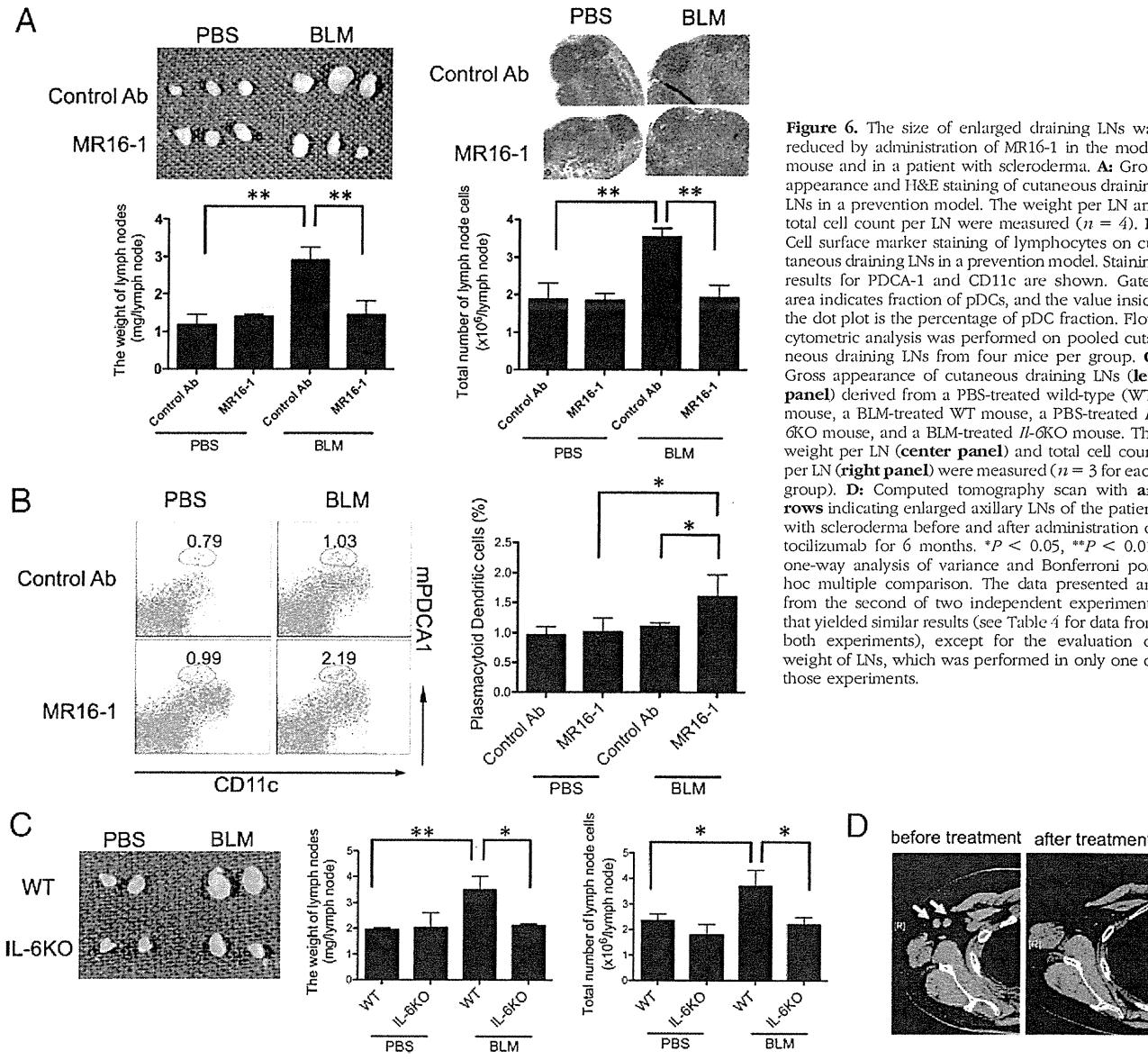

Figure 6. The size of enlarged draining LNs was reduced by administration of MR16-1 in the model mouse and in a patient with scleroderma. **A:** Gross appearance and H&E staining of cutaneous draining LNs in a prevention model. The weight per LN and total cell count per LN were measured ($n = 4$). **B:** Cell surface marker staining of lymphocytes on cutaneous draining LNs in a prevention model. Staining results for PDCA-1 and CD11c are shown. Gated area indicates fraction of pDCs, and the value inside the dot plot is the percentage of pDC fraction. Flow cytometric analysis was performed on pooled cutaneous draining LNs from four mice per group. **C:** Gross appearance of cutaneous draining LNs (**left panel**) derived from a PBS-treated wild-type (WT) mouse, a BLM-treated WT mouse, a PBS-treated *Il-6*KO mouse, and a BLM-treated *Il-6*KO mouse. The weight per LN (**center panel**) and total cell count per LN (**right panel**) were measured ($n = 3$ for each group). **D:** Computed tomography scan with **arrows** indicating enlarged axillary LNs of the patient with scleroderma before and after administration of tocilizumab for 6 months. $^{*}P < 0.05$, $^{**}P < 0.01$, one-way analysis of variance and Bonferroni post hoc multiple comparison. The data presented are from the second of two independent experiments that yielded similar results (see Table 4 for data from both experiments), except for the evaluation of weight of LNs, which was performed in only one of those experiments.

evidence suggest peripheral blood mononuclear cells are a source. The supernatant concentration of IL-6 was reported to be statistically significantly elevated in peripheral blood mononuclear cells[6,20,21] and in T-cell lines[6] derived from patients with systemic sclerosis compared with healthy controls. It also has been reported that experimentally activated B cells might be prone to produce IL-6.[22,23] Other lines of evidence implicate dermal fibroblasts as an important source of IL-6.[13,24–28] In this report, although the expression of IL-6 mRNA in both lesional skin and draining LNs was increased by BLM treatment, the specific cell type producing IL-6 was not identified. Further studies are required to clarify the source(s) of IL-6.

How does secreted IL-6 contribute to the pathogenesis of scleroderma? IL-6 might modulate α-SMA expression in dermal fibroblasts and induce myofibroblasts, which are known to produce collagen[29] and induce sclerotic change.[11,30] We observed IL-6 effects on α-SMA expression from *Il-6*KO dermal fibroblasts *in vitro* in this study (Figure 4A). Unexpectedly, nontreated cultured wild-type dermal fibroblasts strongly expressed α-SMA (Figure 4A), the expression of which was not affected by exogenous IL-6, whereas MR16-1 treatment decreased the expression of α-SMA mRNA (Figure 4, A and B). Therefore, continuous autocrine production of IL-6 by wild-type cultured dermal fibroblasts might increase the threshold for reactivity to IL-6.

Furthermore, in both prevention and treatment protocols with MR16-1, the reduction in dermal sclerosis was accompanied by decreasing numbers of myofibroblasts, which are known as activated fibroblasts with strong fibrogenic property. The absence of myofibroblasts at the BLM injection site of *Il-6*KO mice indicates that IL-6–induced dermal sclerosis occurs via induction of myofibroblasts. Thus, we hypothesize that MR16-1 and tocilizumab have favorable effects on scleroderma via prevention of fibroblast activation. Administration of tocili-

zumab to scleroderma patients exhibited ameliorating effects of skin sclerosis,[15] and seemed to reduce the number of Erk-activated α-SMA–positive fibroblast in lesional skin (Figure 4D). These findings were inconclusive because of the number of cases, and further studies were required.

Another finding was reduction of LN swelling by MR16-1 treatment in mice in the BLM-induced model of scleroderma. We could not determine whether the LN swelling associated with BLM treatment was a cause or effect of BLM-induced skin sclerosis. Examination of the differential ratios of leukocytes, such as T cells, B cells, and macrophages, did not give any insight, as these were not altered after 4 weeks of BLM injection (data not shown). However, there was a slight, but significant, increase in the numbers of cells double-positive for PDCA-1^+CD11c^+ (Figure 6D) or B220$^+$CD11c^+ (data not shown) in the draining LNs of MR16-1–treated mice relative to control Ab–treated mice in the prevention model. This suggests that IL-6 might affect pDC numbers in the LNs. LN swelling is not a well-known symptom in scleroderma, and only a few articles describe LN findings in scleroderma.[31] We should keep an eye on such symptoms.

Recent studies have indicated that pDCs may promote scleroderma via secretion of type 1 interferon,[32] and induction of type 1 interferon was found by anti-topoisomerase antibody-containing serum, but not by anti-centromere antibody.[32,33] However, other data suggest MHC class II–restricted antigen presentation by pDCs might inhibit T-cell–mediated autoimmunity via selective expansion of Ag-specific natural regulatory T cells.[34] Because MHC class II–restricted proliferation of CD4$^+$ T cells had been previously thought to contribute to the pathogenesis of scleroderma,[35] one could speculate that an increased ratio of pDCs might prevent skin sclerosis via regulating peripheral tolerance. However, it is clear that the function of pDCs in pathogenesis of scleroderma is complex and needs further study.

The clear positive effects of IL-6 inhibition in mouse models with scleroderma indicate that further study of IL-6–secreting cells, effectors, and signaling in scleroderma holds great promise for the development of therapies for scleroderma, as well as for other diseases in which IL-6 can play a pivotal role.

Acknowledgments

We thank Prof. Junji Takeda (Osaka University) for expert comments and Dr. Toshiaki Hanafusa, Kenjyu Nishida, and Han Fu for technical assistance.

References

1. Preliminary criteria for the classification of systemic sclerosis (scleroderma). Subcommittee for scleroderma criteria of the American Rheumatism Association Diagnostic and Therapeutic Criteria Committee. Arthritis Rheum 1980, 23:581–590
2. Needleman BW, Wigley FM, Stair RW: Interleukin-1, interleukin-2, interleukin-4, interleukin-6, tumor necrosis factor alpha, and interferon-gamma levels in sera from patients with scleroderma. Arthritis Rheum 1992, 35:67–72
3. Hebbar M, Gillot JM, Hachulla E, Lassalle P, Hatron PY, Devulder B, Janin A: Early expression of E-selectin, tumor necrosis factor alpha, and mast cell infiltration in the salivary glands of patients with systemic sclerosis. Arthritis Rheum 1996, 39:1161–1165
4. Terao M, Murota H, Kitaba S, Katayama I: Tumor necrosis factor-alpha processing inhibitor-1 inhibits skin fibrosis in a bleomycin-induced murine model of scleroderma. Exp Dermatol 2009, 19:38–43
5. Murota H, Hamasaki Y, Nakashima T, Yamamoto K, Katayama I, Matsuyama T: Disruption of tumor necrosis factor receptor p55 impairs collagen turnover in experimentally induced sclerodermic skin fibroblasts. Arthritis Rheum 2003, 48:1117–1125
6. Scala E, Pallotta S, Frezzolini A, Abeni D, Barbieri C, Sampogna F, De Pita O, Puddu P, Paganelli R, Russo G: Cytokine and chemokine levels in systemic sclerosis: relationship with cutaneous and internal organ involvement. Clin Exp Immunol 2004, 138:540–546
7. Yamamoto T, Takagawa S, Katayama I, Yamazaki K, Hamazaki Y, Shinkai H, Nishioka K: Animal model of sclerotic skin. I: local injections of bleomycin induce sclerotic skin mimicking scleroderma, J Invest Dermatol 1999, 112:456–462
8. Yamamoto T, Takagawa S, Katayama I, Nishioka K: Anti-sclerotic effect of transforming growth factor-beta antibody in a mouse model of bleomycin-induced scleroderma. Clin Immunol 1999, 92:6–13
9. Kuwana M, Medsger TA Jr., Wright TM: Analysis of soluble and cell surface factors regulating anti-DNA topoisomerase I autoantibody production demonstrates synergy between Th1 and Th2 autoreactive T cells. J Immunol 2000, 164:6138–6146
10. Kishimoto T: The biology of interleukin-6. Blood 1989, 74:1–10
11. Gallucci RM, Lee EG, Tomasek JJ: IL-6 modulates alpha-smooth muscle actin expression in dermal fibroblasts from IL-6-deficient mice. J Invest Dermatol 2006, 126:561–568
12. Duncan MR, Berman B: Stimulation of collagen and glycosaminoglycan production in cultured human adult dermal fibroblasts by recombinant human interleukin 6. J Invest Dermatol 1991, 97:686–692
13. Kawaguchi Y, Hara M, Wright TM: Endogenous IL-1alpha from systemic sclerosis fibroblasts induces IL-6 and PDGF-A. J Clin Invest 1999, 103:1253–1260
14. Nishimoto N, Kishimoto T: Interleukin 6: from bench to bedside. Nat Clin Pract Rheumatol 2006, 2:619–626
15. Shima Y, Kuwahara Y, Murota H, Kawai M, Hirano T, Arimitsu J, Narazaki M, Hagihara K, Ogata A, Katayama I, Kawase I, Kishimoto T, Tanaka T: The skin of patients with systemic sclerosis softened during the treatment with anti-IL-6 receptor antibody tocilizumab. Rheumatology 2010, 49:2408–12
16. Gallucci RM, Sloan DK, Heck JM, Murray AR, O'Dell SJ: Interleukin 6 indirectly induces keratinocyte migration. J Invest Dermatol 2004, 122:764–772
17. Kopf M, Baumann H, Freer G, Freudenberg M, Lamers M, Kishimoto T, Zinkernagel R, Bluethmann H, Kohler G: Impaired immune and acute-phase responses in interleukin-6-deficient mice. Nature 1994, 368:339–342
18. Takagi N, Mihara M, Moriya Y, Nishimoto N, Yoshizaki K, Kishimoto T, Takeda Y, Ohsugi Y: Blockage of interleukin-6 receptor ameliorates joint disease in murine collagen-induced arthritis. Arthritis Rheum 1998, 41:2117–2121
19. Kuwahara Y, Shima Y, Shirayama D, Kawai M, Hagihara K, Hirano T, Arimitsu J, Ogata A, Tanaka T, Kawase I: Quantification of hardness, elasticity and viscosity of the skin of patients with systemic sclerosis using a novel sensing device (Vesmeter): a proposal for a new outcome measurement procedure. Rheumatology (Oxford) 2008, 47: 1018–1024
20. Hasegawa M, Sato S, Ihn H, Takehara K: Enhanced production of interleukin-6 (IL-6), oncostatin M and soluble IL-6 receptor by cultured peripheral blood mononuclear cells from patients with systemic sclerosis. Rheumatology (Oxford) 1999, 38:612–617
21. Crestani B, Seta N, De Bandt M, Soler P, Rolland C, Dehoux M, Boutten A, Dombret MC, Palazzo E, Kahn MF, et al.: Interleukin 6 secretion by monocytes and alveolar macrophages in systemic sclerosis with lung involvement. Am J Respir Crit Care Med 1994, 149: 1260–1265
22. Saito E, Fujimoto M, Hasegawa M, Komura K, Hamaguchi Y, Kaburagi Y, Nagaoka T, Takehara K, Tedder TF, Sato S: CD19-dependent B lymphocyte signaling thresholds influence skin fibrosis and

autoimmunity in the tight-skin mouse. J Clin Invest 2002, 109:1453–1462
23. Matsushita T, Hasegawa M, Yanaba K, Kodera M, Takehara K, Sato S: Elevated serum BAFF levels in patients with systemic sclerosis: enhanced BAFF signaling in systemic sclerosis B lymphocytes. Arthritis Rheum 2006, 54:192–201
24. Takemura H, Suzuki H, Fujisawa H, Yuhara T, Akama T, Yamane K, Kashiwagi H: Enhanced interleukin 6 production by cultured fibroblasts from patients with systemic sclerosis in response to platelet derived growth factor. J Rheumatol 1998, 25:1534–1539
25. Kawaguchi Y, Nishimagi E, Tochimoto A, Kawamoto M, Katsumata Y, Soejima M, Kanno T, Kamatani N, Hara M: Intracellular IL-1alpha-binding proteins contribute to biological functions of endogenous IL-1alpha in systemic sclerosis fibroblasts, Proc Natl Acad Sci U S A 2006, 103:14501–14506
26. Fukasawa C, Kawaguchi Y, Harigai M, Sugiura T, Takagi K, Kawamoto M, Hara M, Kamatani N: Increased CD40 expression in skin fibroblasts from patients with systemic sclerosis (SSc): role of CD40-CD154 in the phenotype of SSc fibroblasts. Eur J Immunol 2003, 33:2792–2800
27. Kadono T, Kikuchi K, Ihn H, Takehara K, Tamaki K: Increased production of interleukin 6 and interleukin 8 in scleroderma fibroblasts. J Rheumatol 1998, 25:296–301
28. Koch AE, Kronfeld-Harrington LB, Szekanecz Z, Cho MM, Haines GK, Harlow LA, Strieter RM, Kunkel SL, Massa MC, Barr WG, Jimenez SA: In situ expression of cytokines and cellular adhesion molecules in the skin of patients with systemic sclerosis. Their role in early and late disease. Pathobiology 1993, 61:239–246
29. Wynn TA: Cellular and molecular mechanisms of fibrosis. J Pathol 2008, 214:199–210
30. Kirk TZ, Mark ME, Chua CC, Chua BH, Mayes MD: Myofibroblasts from scleroderma skin synthesize elevated levels of collagen and tissue inhibitor of metalloproteinase (TIMP-1) with two forms of TIMP-1. J Biol Chem 1995, 270:3423–3428
31. Ofstad E: Scleroderma (progressive systemic sclerosis). A case involving polyneuritis and swelling of the lymph nodes. Acta Rheumatol Scand 1960, 6:65–75
32. Eloranta ML, Franck-Larsson K, Lovgren T, Kalamajski S, Ronnblom A, Rubin K, Alm GV, Ronnblom L: Type I interferon system activation and association with disease manifestations in systemic sclerosis. Ann Rheum Dis 2010, 69:1396–1402
33. Kim D, Peck A, Santer D, Patole P, Schwartz SM, Molitor JA, Arnett FC, Elkon KB: Induction of interferon-alpha by scleroderma sera containing autoantibodies to topoisomerase I: association of higher interferon-alpha activity with lung fibrosis. Arthritis Rheum 2008, 58: 2163–2173
34. Irla M, Kupfer N, Suter T, Lissilaa R, Benkhoucha M, Skupsky J, Lalive PH, Fontana A, Reith W, Hugues S: MHC class II-restricted antigen presentation by plasmacytoid dendritic cells inhibits T cell-mediated autoimmunity. J Exp Med 2010, 207:1891–1905
35. Kuwana M, Medsger TA Jr., Wright TM: T cell proliferative response induced by DNA topoisomerase I in patients with systemic sclerosis and healthy donors. J Clin Invest 1995, 96:586–596

A Novel Application of Topical Rapamycin Formulation, an Inhibitor of mTOR, for Patients With Hypomelanotic Macules in Tuberous Sclerosis Complex

Tuberous sclerosis complex (TSC) is an autosomal dominant disease characterized by systemic hamartomas. Two genes, *TSC1* and *TSC11*, which encode hamartin and tuberin, are responsible for TSC. The complex of hamartin and tuberin inhibits the mammalian target of rapamycin (mTOR),[1] which has numerous functions in the regulation of protein synthesis and cell growth. The constitutive activation of mTOR is associated with abnormal cellular proliferation, which causes TSC-related hamartomas.

Recent reports suggest that inhibitors of mTOR, such as rapamycin, may be effective for the treatment of TSC-related tumorigenesis, including facial angiofibroma.[2,3] However, the efficacy of rapamycin for hypomelanotic macules is still unknown. We herein report 2 cases of hypomelanotic macules in TSC successfully treated with a topical rapamycin, 0.2%, formulation.

Report of Cases. *Case 1.* An 8-year-old boy presented with facial angiofibromas, multiple hypomelanotic macules, and shagreen patches. He had epilepsy but no mental abnormalities and showed cortical tubers and subependymal nodules on brain magnetic resonance imaging (MRI). The hypomelanotic macule and angiofibromas on the face were treated with rapamycin gel, 0.2% twice a day for 12 weeks.

Case 2. A 2-year-old boy presented with skin symptoms similar to those in case 1, refractory epilepsy, mental retardation, and cortical tubers on brain MRI. The hy-

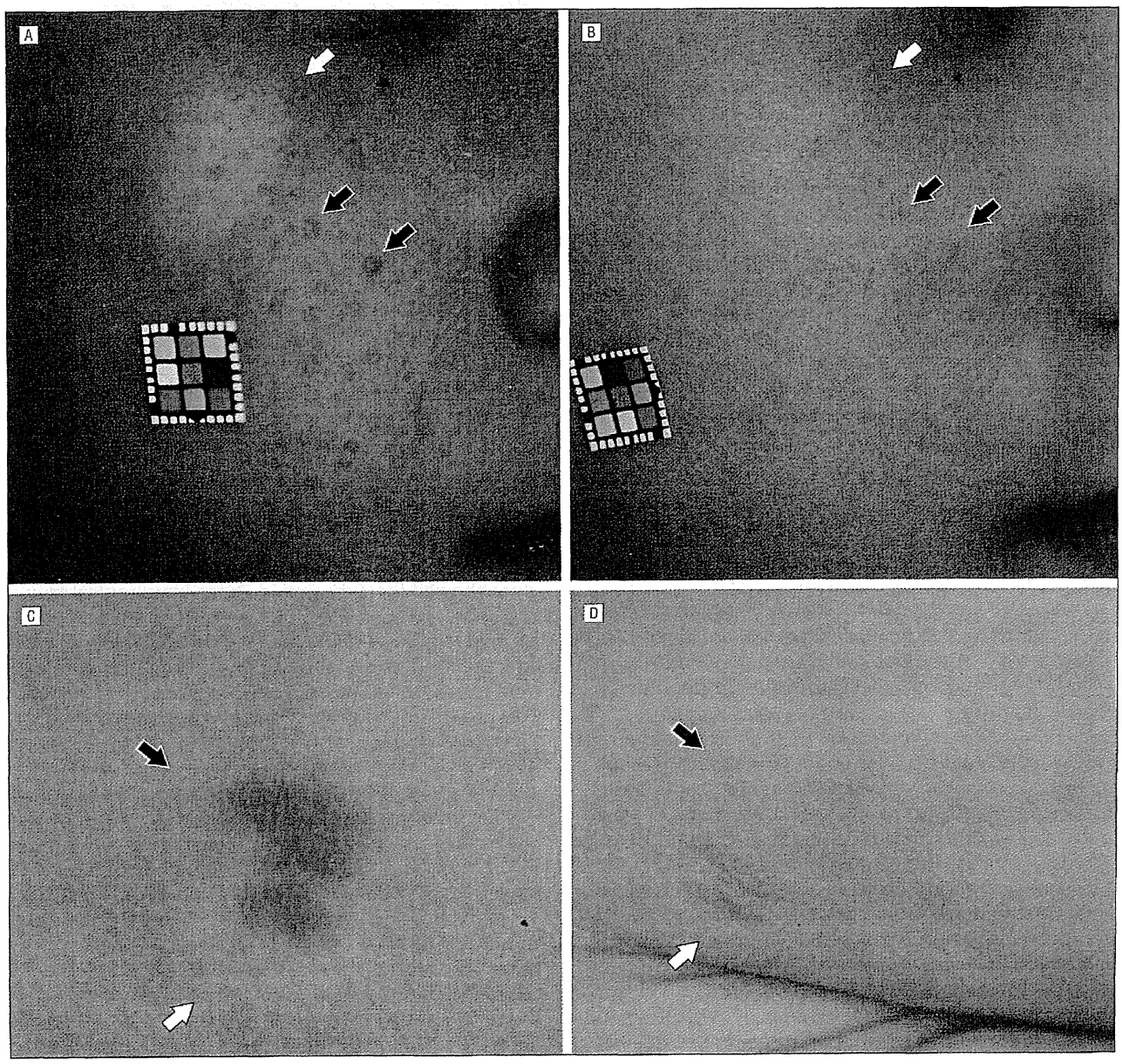

Figure. Clinical images. Hypomelanotic macules (white arrows) before treatment (A and C) disappeared after treatment with rapamycin gel, 0.2% (B) and ointment (D). Both angiofibromas (A) and red plaque (C) (black arrows) were reduced by the rapamycin treatments (B and D).

pomelanotic macule and red plaque on the face were treated in the same manner, using rapamycin, 0.2% ointment.

Both cases were sporadic cases and were diagnosed as definitive TSC according to Roach's clinical diagnostic criteria[4] and had no treatment before the rapamycin treatment. At the end of the treatment, the hypomelanotic macules in both cases were improved, with no difference in efficacy with regard to their different phenotypes. The angiofibroma in case 1 and red plaque in case 2 also improved (**Figure**). No adverse effects were observed by laboratory tests or on the skin, and the serum rapamycin concentrations were under the detection limit (0.3 ng/mL). Three months after stopping the treatment, only the angiofibromas recurred in case 1, while hypomelanotic macules also slightly recurred with red plaque in case 2.

This study was approved by the ethics committee of Osaka University Faculty of Medicine, and informed consents were obtained from all patients.

Comment. The pathogenesis of hypomelanotic macules due to TSC has not yet been well investigated. One histologic investigation showed that hypomelanotic macules due to TSC have a normal number of melanocytes with poorly developed dendritic processes and that the melanosomes decrease in number, size, and melanization.[5] Hypomelanotic macules due to TSC may arise from abnormal melanization or melanin transport. Rapamycin has been shown to increase the transcription of microphthalmia transcription factor (MITF), which is implicated in melanogenic gene expression, and to induce melanization in melanoma cells.[6] Therefore, the topical application of rapamycin for hypomelanotic macules due to TSC seems to be a rational and effective treatment strategy.

Based on our findings, topical rapamycin formulation appears to be a useful and safe treatment for the hypomelanotic macules arising in patients with TSC. Our result also indicates a novel function of mTOR in melanocytes and a new clinical application for rapamycin.

Mari Wataya-Kaneda, MD, PhD
Mari Tanaka, MD
Ayumi Nakamura, BPharm
Shoji Matsumoto, PhD
Ichiro Katayama, MD, PhD

Author Affiliations: Department of Dermatology, Graduate School of Medicine, Osaka University (Drs Wataya-Kaneda, Tanaka, and Katayama), and Department of Pharmacy, Osaka University Hospital (Drs Nakamura and Matsumoto), Osaka, Japan.
Correspondence: Dr Wataya-Kaneda, Department of Dermatology, Graduate School of Medicine, Osaka University, 2-2 Yamada-oka, Suita, Osaka 565-0871, Japan (mkaneda@derma.med.osaka-u.ac.jp).
Financial Disclosure: None reported.
Funding/Support: This work was supported by the grant from the Ministry of Education, Culture, Sports, Science and Technology of Japan and the grant from the Ministry of Health, Labor and Welfare of Japan.

1. Inoki K, Li Y, Zhu T, Wu J, Guan KL. TSC2 is phosphorylated and inhibited by Akt and suppresses mTOR signalling. *Nat Cell Biol*. 2002;4(9):648-657.
2. Franz DN, Leonard J, Tudor C, et al. Rapamycin causes regression of astrocytomas in tuberous sclerosis complex. *Ann Neurol*. 2006;59(3):490-498.
3. Haemel AK, O'Brian AL, Teng JM. Topical rapamycin: a novel approach to facial angiofibromas in tuberous sclerosis. *Arch Dermatol*. 2010;146(7):715-718.
4. Roach ES, Gomez MR, Northrup H. Tuberous sclerosis complex consensus conference: revised clinical diagnostic criteria. *J Child Neurol*. 1998;13(12):624-628.
5. Jimbow K, Fitzpatrick TB, Szabo G, Hori Y. Congenital circumscribed hypomelanosis: a characterization based on electron microscopic study of tuberous sclerosis, nevus depigmentosus, and piebaldism. *J Invest Dermatol*. 1975;64(1):50-62.
6. Oiguchi K, Banno Y, Nakagawa Y, Akao Y, Nozawa Y. Negative regulation of melanogenesis by phospholipase D1 through mTOR/p70 S6 kinase 1 signaling in mouse B16 melanoma cells. *J Cell Physiol*. 2005;205(3):444-451.

Atypical Gingivitis Heralding a Case of Orofacial Granulomatosis

Orofacial granulomatosis is a disorder of the orofacial soft tissues characterized clinically by recurrent to persistent lip and facial swelling and histopathologically by noncaseating granulomatous inflammation, lymphangiectasia, and perivascular lymphocytic inflammation.[1,2] It is a diagnosis of exclusion considered to represent a spectrum of clinical entities including cheilitis granulomatosa and Melkersson-Rosenthal syndrome. We describe herein a case of granulomatous stomatitis presenting with atypical gingivitis consistent with orofacial granulomatosis. Since granulomatous stomatitis may be a marker for systemic disease, it is imperative to rule out other potentially associated conditions.

Report of a Case. A 60-year-old white woman presented with a 3-year history of tender, swollen gums and progressive hoarseness. She denied a history of atopy and was unaware of a food that exacerbated the symptoms. Removal of gingival tissue during a debulking procedure showed focal erosion, a dense lymphoplasmacytic infiltrate, and scattered noncaseating granulomas on histopathologic analysis. Over the previous 5 months, she had experienced uncomfortable swelling of her left buccal mucosa in addition to ongoing gingivitis. The presumptive diagnosis was foreign-body gingivitis.

On physical examination, no facial palsy was noted. The left buccal mucosa was boggy with orange-yellow discoloration, and the attached gingiva showed mild erythema (**Figure 1**). With nasolaryngoscopy, an exophytic mass was apparent on the anterior commissure of the vocal cords. This was subsequently found to be a squamous papilloma (believed to be unrelated). Gingival and mucosal biopsy specimens showed focal lichenoid mucositis with submucosal noncaseating granulomas suggestive of sarcoid (**Figure 2**). No foreign body was detected, and findings of periodic acid–Schiff diastase, Grocott methenamine-silver, and acid-fast bacilli stains; tissue cultures; and direct immunofluorescence studies were all negative. Inflammatory bowel disease was excluded through normal or negative findings of

BJD
British Journal of Dermatology

A topical combination of rapamycin and tacrolimus for the treatment of angiofibroma due to tuberous sclerosis complex (TSC): a pilot study of nine Japanese patients with TSC of different disease severity

M. Wataya-Kaneda, M. Tanaka, A. Nakamura,* S. Matsumoto* and I. Katayama

Department of Dermatology, Graduate School of Medicine, Osaka University, 2-2 Yamada-oka, Suita, Osaka 565-0871, Japan
**Department of Pharmacy, Osaka University Hospital, Osaka, Japan*

Summary

Background Dysregulation of mTOR signalling by mutations in tuberin and/or hamartin leads to the formation of tuberous sclerosis complex (TSC). Trials to treat TSC using mTOR inhibitors, including rapamycin, have been performed. Although rapamycin improves many TSC lesions, significant side-effects appear after systemic administration. Topical administration has been recommended.

Objectives The efficacy of rapamycin–tacrolimus ointment was examined for TSC-related angiofibroma.

Methods Left–right comparisons of the tacrolimus ointments with/without 0·2% rapamycin was conducted in symmetrical facial angiofibromas in nine patients with definitive TSC. After the 3-month treatment, a cumulative score for redness, flatness and papule size was used to evaluate the efficacy of the treatment. Blood rapamycin levels were analysed by liquid chromatography-electrospray mass spectrometry (LC-ESI/MS).

Results At the end of the treatment, all of the scores significantly improved for rapamycin–tacrolimus treatment compared with tacrolimus alone. No adverse reactions were noted and blood levels of rapamycin were below the detection limit in all cases.

Conclusions Topical application of rapamycin–tacrolimus ointment is a safe and useful treatment for TSC-related angiofibroma.

Correspondence
Mari Wataya-Kaneda.
E-mail: mkaneda@derma.med.osaka-u.ac.jp

Accepted for publication
3 June 2011

Funding sources
Funded by a grant from the Ministry of Education, Culture, Sports, Science and Technology of Japan and a grant from the Ministry of Health, Labour and Welfare of Japan.

Conflicts of interest
None declared.

DOI 10.1111/j.1365-2133.2011.10471.x

Tuberous sclerosis complex (TSC) is an autosomal dominant disease characterized by hamartomas. Two genes, TSC1[1] and TSC2,[2] encoding hamartin and tuberin, are responsible for TSC. Hamartin and tuberin are physically associated *in vivo*, are active in the same complex, and inhibit the mammalian target of rapamycin (mTOR).[3] Mutations of TSC1 or TSC2 cause abnormalities in hamartin or tuberin, resulting in the defects in mTOR signalling inhibition. mTOR is a protein kinase with many functions in protein synthesis and growth. The constitutive activation of mTOR is associated with abnormal cellular proliferation, which occurs in TSC-related hamartomas.

These observations suggest that mTOR inhibitors, such as rapamycin, may represent a new therapy for TSC. Oral administration of rapamycin was effective for astrocytomas, renal angiomyolipomas, lymphangioleiomyomatosis and facial angiofibromas associated with TSC.[4–9] Although the oral administration of rapamycin reduced the tumours, many side-effects developed, and re-growth of the tumours occurred after discontinuing administration. Therefore, the topical administration of rapamycin is recommended for skin lesions. Although 1% rapamycin ointment has been reported to be effective in one case of TSC-related angiofibroma,[9] another case needed co-treatment with orally administered rapamycin.[10] Further evaluation of the topical treatment in patients with TSC is necessary.

Rapamycin is a large molecule, and it is difficult to make an easily absorbed ointment. Tacrolimus is similar to rapamycin in its structure. Tacrolimus and rapamycin bind to FK-binding protein 12 (FKBP12) in a competitive manner. The complex of tacrolimus and FKBP12 functions as a calcineurin inhibitor, while the complex of rapamycin and FKBP12 functions as an mTOR inhibitor. In this study, rapamycin was mixed in 0·03% tacrolimus ointment (Protopic®; Astellas, Tokyo, Japan).

Materials and methods

We developed a 0·2% rapamycin ointment by mixing Rapamune® (rapamycin for internal use; Pfizer, New York,

© 2011 The Authors

Table 1 Patients with tuberous sclerosus complex (TSC) who participated in the rapamycin ointment therapy and their final, end point score

Patient no.	Sex	Age	Familial	Geno type	Neural symptoms (autism/mental retardation)	Epilepsy	MRI evidence		Renal involvement	Pulmonary involvement	Property/ shape/size of the skin lesions	Severity of skin lesions	Colour of skin lesions	Speed of new appearance and growth	Final score[a]
							Cortical tuber	SEN							
1	M	20	Sporadic	*TSC2*	+	Y	Y	Y	Cyst	MMPH	Papule	Medium	Red	Moderate	2
2	M	9	Sporadic	ND	−	Y	Y	N	Cyst	ND	Papule	Medium	Red	High	4
3[b]	F	30	Sporadic	*TSC2*	−	Y	Y	Y	AML	LAM	Plaque	Severe	Red	Moderate	2
4	M	11	Sporadic	*TSC1*	A+	Y	Y	Y	N	ND	Papule	Medium	Normal skin colour	Moderate	3
5	F	14	Sporadic	NMF	A+	Y	Y	Y	AML	ND	Papule	Medium	Red	Slight	2
6	F	46	Sporadic	*TSC2*	+	Y	Y	Y	AML	LAM	Papule, erythema	Medium	Red	Slight	2
7[b]	F	38	Sporadic	ND	−	Y	Y	Y	AML	LAM, MMPH	Papule, nodule	Medium	Red	Moderate	3
8	F	11	Sporadic	NMF	A++	Y	Y	Y	N	ND	Small papule	Slight	Red	High	4
9[b]	F	17	Sporadic	NMF	A++	Y	Y	Y	AML cyst	NF	Plaque	Severe	Red	Moderate	1·5

−, no mental retardation; +, slight mental retardation; ++, severe mental retardation; A, autism; AML, renal angiomyolipomas; LAM, lymphangioleiomyomatosis; MMPH, multifocal micronodular pneumocyte hyperplasia; MRI, magnetic resonance imaging; N, no; ND, not done (genotyping or pulmonary testing); NF, no evidence of LAM and MMPH was found in spite of pulmonary examinations; NMF, no mutation found in either *TSC1* or *TSC2* gene; SEN, subependymal nodule; Y, yes. [a]To assess the target lesions, a cumulative sign score of target angiofibromas on a scale of 0–4 for redness, flatness and papule size was used. A > 80% improvement of redness, thickening and papule size received a score of two points, a 50–80% improvement was defined as one point, and a 20–50% improvement was given 0·5 points. The total of each score assessed by two independent evaluators was added to provide the cumulative score. The final score in the far right column is the average of the total score of the size, redness and flatness. [b]Patient is shown in Figure 2.

© 2011 The Authors
BJD © 2011 British Association of Dermatologists 2011 **165**, pp912–916

NY, U.S.A.) in 0·03% tacrolimus ointment as a vehicle. Nine patients, three males and six females, aged 9–46 years, diagnosed with definitive TSC according to the clinical diagnostic criteria of Roach *et al.*[11] were enrolled in this study. A left–right comparison of 0·03% tacrolimus ointment with/without 0·2% rapamycin was conducted in the nine patients with TSC with symmetrical facial angiofibroma (Table 1). Each angiofibroma of 20 cm^2 was treated with the ointments twice daily after tape stripping for 3 months. In all patients, haematological and biochemical examinations were done before and after treatment. Blood rapamycin levels were analysed by Liquid chromatography – electrospray ionization mass spectrometry (detection limit: 0·3 ng mL^{-1}) after treatment. Patients were assessed at 0, 2, 6 and 12 weeks during treatment as shown in Figure 1.

This study was approved by the ethics committee of Osaka University Faculty of Medicine and was disclosed to the University Hospital Medical Information Network. Informed consent was obtained from all patients.

Data were analysed with Student's t-test for paired data.

Results

Patient information and the scores at the end of the topical combination therapy are shown in Table 1. We assessed all the items at each time point (Fig. 1). All the scores at the end of the combination treatment with rapamycin and tacrolimus significantly improved compared with the side treated with tacrolimus alone. In patients 2 and 8, in whom the initial angiofibroma was slight, almost all the papules disappeared

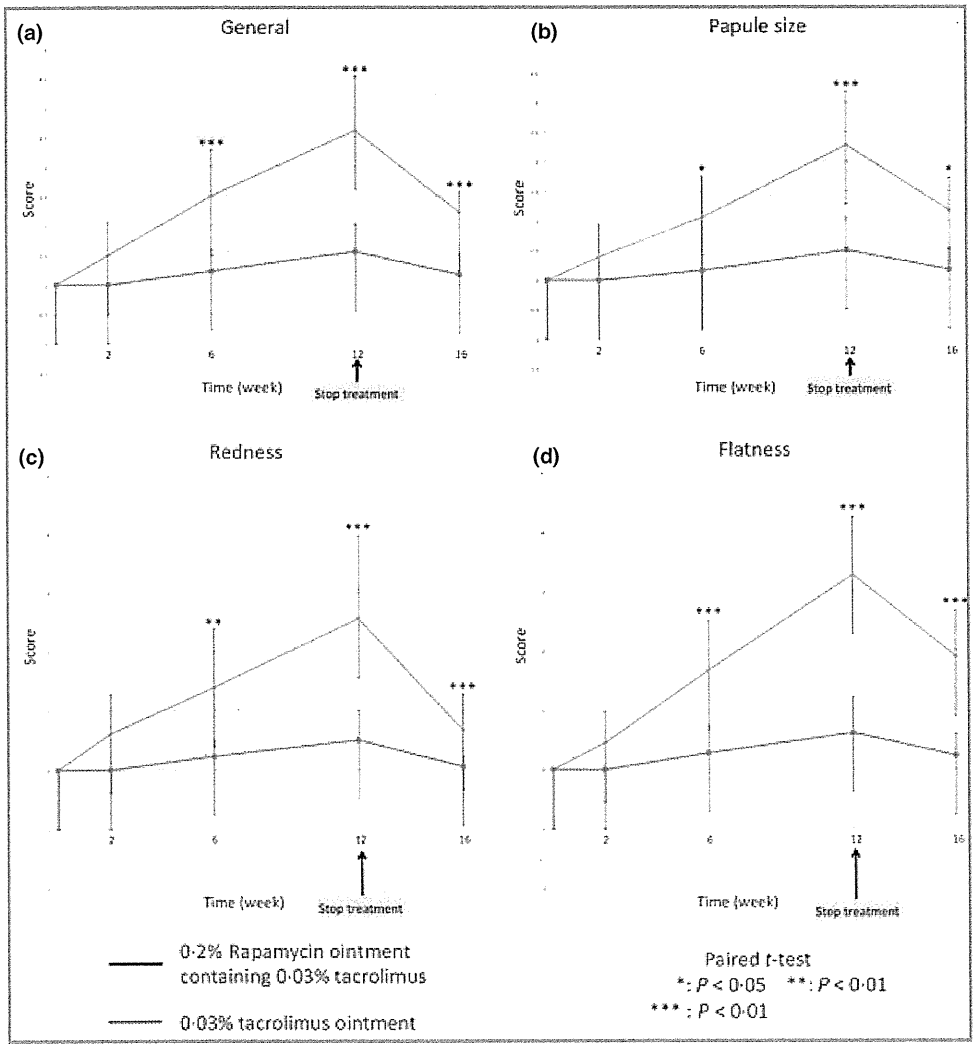

Fig 1. The effects on angiofibromas at each time point of 0·2% rapamycin ointment containing 0·03% tacrolimus or control ointment containing 0·03% tacrolimus were assessed by scoring the papule size (b), redness (c) and flatness (d) of the lesions. The general score (a) was the average of the total score of the size, redness and flatness. To assess the target lesions, a cumulative sign score of target angiofibromas on a scale of 0–4 for redness, flatness and papule size was used. A > 80% improvement of redness, thickening and papule size received a score of two points, a 50–80% improvement was defined as one point, and a 20–50% improvement was given 0.5 points. The totals of each score assessed by two independent evaluators were added to provide the cumulative score. Each point shows the mean ± standard deviation of the score of nine patients. Statistical significance was determined as *P < 0·05, **P < 0·01 and ***P < 0·001.

© 2011 The Authors

completely. In patients 1, 4 and 7, many papules either disappeared or diminished. In patients 3 and 9, many plaques diminished, although the scores were not very high because the initial tumour volumes were large. Conversely, patients 5 and 6 showed only mild effects (Table 1). Representative photographs of patients 3, 7 and 9 are shown in Figure 2.

All symptoms, except papule size, began to improve during the 6th week after treatment started. Flatness improved the most. One month after stopping the treatment, redness increased to 60–80% of baseline, but the reduction of papule size and flatness continued. Tacrolimus alone induced a little improvement in angiofibroma, but the efficacy was much lower than that of the combination treatment, and the scores returned to the baseline 1 month after stopping the treatment (Fig. 1).

None of the patients suffered from contact dermatitis or had abnormal laboratory results (data not shown). Blood levels of rapamycin were below the detection limit in all cases.

Discussion

The rapamycin–tacrolimus ointment had a significant effect on TSC angiofibroma, and was more effective than tacrolimus alone (Fig. 1). When we treated patients with facial angiofibro-

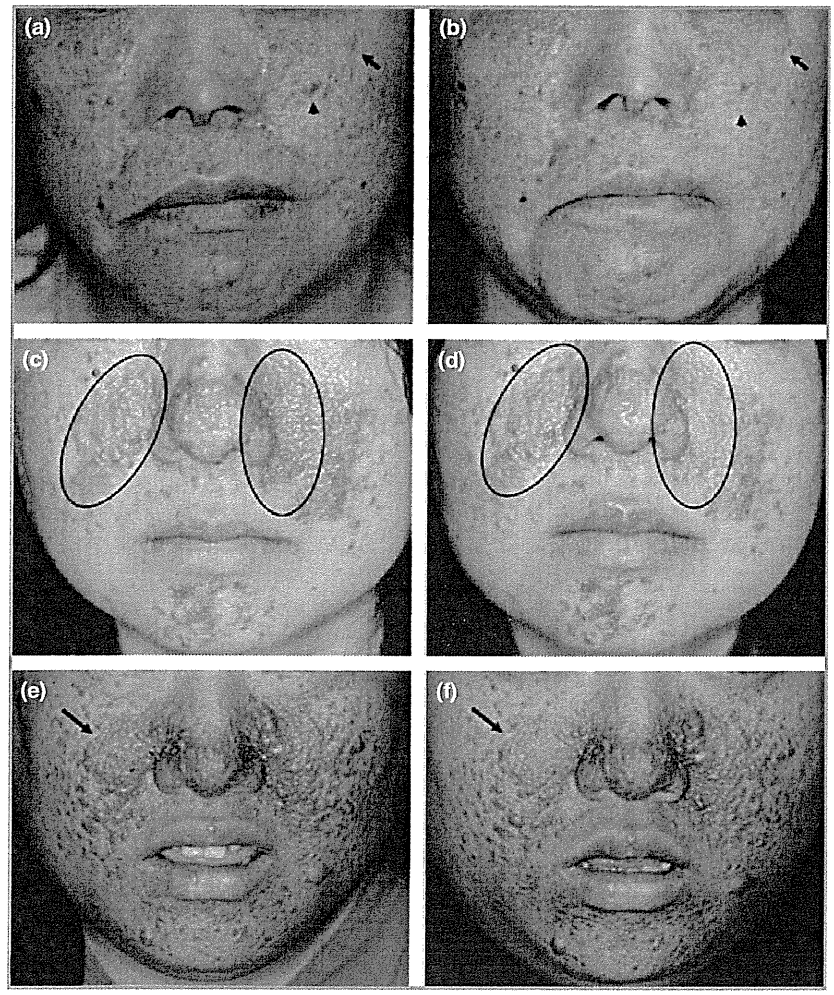

Fig 2. Angiofibromas in patients no. 7 (a, b), no. 3 (c, d) and no. 9 (e, f). (a) Angiofibroma was seen on both cheeks before the treatment. Typical papules (arrowhead) and redness (arrow) were detected on the left cheek before treatment. (b) Twelve weeks after starting the treatment, the angiofibroma on the left cheek (treated with the rapamycin–tacrolimus ointment) was reduced compared with that on the right cheek treated with tacrolimus ointment. A dramatic reduction of the papule size (arrowhead) and redness (arrow) was achieved by the rapamycin–tacrolimus ointment. (c) A typical butterfly-shaped angiofibroma was seen on the nose and cheeks before treatment. The circle indicates the area of topical treatment with the tacrolimus ointment alone (right cheek) and rapamycin–tacrolimus ointment (left cheek). (d) Twelve weeks after the treatment, the angiofibroma on the left side was improved, especially in terms of the redness, by the rapamycin–tacrolimus ointment. The improvement was restricted to the area treated with the rapamycin–tacrolimus ointment. (e) A typical butterfly-shaped angiofibroma was distributed from the nose to both cheeks before treatment. The arrow indicates a typical plaque of angiofibroma on the right cheek before the treatment. (f) Twelve weeks after initiating the treatment, the plaque of the angiofibroma on the right cheek treated with the rapamycin–tacrolimus ointment was improved, especially in terms of the size and flatness of the papules. The arrow indicates the improvement of the plaque by the rapamycin–tacrolimus ointment.

© 2011 The Authors

mas using 0·03% tacrolimus ointment in the past, no improvement was observed. Therefore, some of the improvement of the angiofibroma noted as due to the tacrolimus alone may have been due to the stripping, not to the effects of tacrolimus. However, it is possible that the combination of rapamycin and tacrolimus may have led to synergistic activity, as the efficacy of rapamycin alone was not evaluated. It will be necessary to make an effective vehicle without tacrolimus to address this concern.

The topical combination treatment was effective in all nine patients. Patients with rapidly growing tumours seemed to respond better to the treatment. No other factors appeared to affect the efficacy of the treatment on the skin symptoms, although age may also have a minimal effect on the efficacy (Table 1). One month after stopping the treatment, all of the symptoms recurred (especially the redness), although they did not return to baseline levels (Fig. 1).

There were no side-effects or abnormal laboratory data, and no transfer of rapamycin to the blood, in any of the nine patients. Considering these results, the topical combination therapy of rapamycin and tacrolimus appears to be safe and effective for the treatment of TSC-related angiofibroma.

Topical combination therapy also represents a promising treatment for skin lesions of mTOR-related neurocutaneous syndromes, such as neurofibromatosis type 1,[12] Birt–Hogg–Dubé syndrome[13] and Cowden syndrome.[14]

What's already known about this topic?

- Generalized administration of rapamycin is effective for tuberous sclerosis complex (TSC) lesions, but causes side-effects.
- Topical treatment using 1% rapamycin ointment was effective in one patient with TSC angiofibroma.

What does this study add?

- Left–right comparison of tacrolimus ointment with/without 0·2% rapamycin was conducted in symmetrical facial angiofibromas of nine patients with TSC with different symptoms.
- Rapamycin–tacrolimus ointment was significantly more effective in all patients, with fewer side-effects, and more effective for growing tumours.

References

1 van Slegtenhorst M, de Hoogt R, Hermans C *et al.* Identification of the tuberous sclerosis gene TSC1 on chromosome 9q34. *Science* 1997; **277**:805–8.

2 European Chromosome 16 Tuberous Sclerosis Consortium. Identification and characterization of the tuberous sclerosis gene on chromosome 16. *Cell* 1993; **75**:1305–15.

3 Inoki K, Li Y, Xu T, Guan KL. Rheb GTPase is a direct target of TSC2 GAP activity and regulates mTOR signaling. *Genes Dev* 2003; **17**:1829–34.

4 Franz DN, Leonard J, Tudor C *et al.* Rapamycin causes regression of astrocytomas in tuberous sclerosis complex. *Ann Neurol* 2006; **59**:490–8.

5 Herry I, Neukirch C, Debray MP *et al.* Dramatic effect of sirolimus on renal angiomyolipomas in a patient with tuberous sclerosis complex. *Eur J Intern Med* 2007; **18**:76–7.

6 Taille C, Debray MP, Crestani B. Sirolimus treatment for pulmonary lymphangioleiomyomatosis. *Ann Intern Med* 2007; **146**:687–8.

7 Bissler JJ, McCormack FX, Young LR *et al.* Sirolimus for angiomyolipoma in tuberous sclerosis complex or lymphangioleiomyomatosis. *N Engl J Med* 2008; **358**:140–51.

8 Hofbauer GF, Marcollo-Pini A, Corsenca A *et al.* The mTOR inhibitor rapamycin significantly improves facial angiofibroma lesions in a patient with tuberous sclerosis. *Br J Dermatol* 2008; **159**:473–5.

9 Haemel AK, O'Brian AL, Teng JM. Topical rapamycin: a novel approach to facial angiofibromas in tuberous sclerosis. *Arch Dermatol* 2010; **146**:715–18.

10 Kaufman McNamara E, Curtis AR, Fleischer AB Jr. Successful treatment of angiofibromata of tuberous sclerosis complex with rapamycin. *J Dermatolog Treat* 2010 [Epub ahead of print]

11 Roach ES, Gomez MR, Northrup H. Tuberous sclerosis complex consensus conference: revised clinical diagnostic criteria. *J Child Neurol* 1998; **13**:624–8.

12 Brems H, Beert E, de Ravel T, Legius E. Mechanisms in the pathogenesis of malignant tumours in neurofibromatosis type 1. *Lancet Oncol* 2009; **10**:508–15.

13 Menko FH, van Steensel MA, Giraud S *et al.* Birt–Hogg–Dubé syndrome: diagnosis and management. *Lancet Oncol* 2009; **10**:1199–206.

14 Blumenthal GM, Dennis PA. PTEN hamartoma tumor syndromes. *Eur J Hum Genet* 2008; **16**:1289–300.

© 2011 The Authors

Journal of Dermatological Science xxx (2011) xxx–xxx

Contents lists available at SciVerse ScienceDirect

Journal of Dermatological Science

journal homepage: www.elsevier.com/jds

Letter to the Editor

Repigmentation of leukoderma in a piebald patient associated with a novel *c-KIT* gene mutation, G592E, of the tyrosine kinase domain

Piebaldism (MIM 172800) is an autosomal dominant disorder showing localized poliosis and leukoderma of the frontal scalp, forehead, ventral trunk, and extremities. On the other hand, vitiligo is an acquired pigmentation disease, and the white patches distributed typically in an acral and periorificial regions. The depigmented regions have been believed to be stable with piebaldism because of the congenital absence of melanocytes in those regions involved, whereas, the size and the distribution of depigmented macules alters in vitiligo by a selective destruction of the melanocytes.

The *c-KIT* gene is located on chromosome 4q12 and encodes a type III tyrosine kinase receptor, c-KIT. The c-KIT protein functions as a receptor for stem cell factor (SCF), and mutations of the *c-KIT* gene are identified in 75% of subjects with piebaldism [1,2]. This c-KIT–SCF interaction is essential for melanocyte development, proliferation, survival, and migration. The binding of SCF to c-KIT initiates dimerization of c-KIT, which induces transactivation and auto-phosphorylation of tyrosine residues within the intracellular tyrosine kinase domains, followed by binding of signal transduction molecules [3]. Accordingly, mutations within the tyrosine kinase domain induce a severe phenotype of piebaldism because of their dominant negative effect [4]. A large number of subjects with piebaldism have intracellular mutations of *c-KIT*, and most of the patients with these mutations have severe phenotypes. On the other hand, there are several flame shift mutations and certain intracellular point mutations investigated with moderate phenotype including recent reports [5–7].

A 5-year-old Japanese female had a white section of hair in the front of her scalp, and leukoderma on her frontal scalp, forehead, abdomen, and knees. She also had hyperpigmented macules on her trunk and frontal thighs (Fig. 1). Her 35-year-old father had both leukoderma and hyperpigmentation with similar distributions (data not shown). We found progressive repigmentation within the leukoderma region on the patient's knees during inspections performed at 2 year intervals (Fig. 1). Her father had also inquired about progressive repigmentation within his leukoderma around his knees.

The parents provided written informed consent for their daughter's participation, and the study was approved by the Genetic Ethics Committee of Kinki University. We amplified the *c-KIT* gene by polymerase chain reaction (PCR) from genomic DNA of peripheral blood leukocytes obtained from the patient and her father, and the nucleic acid sequence of the *c-KIT* gene was analyzed by direct sequencing [5]. The identified mutation in *c-KIT* was confirmed by three independent sequencing reactions from the patient's DNA and one sequencing study of her father's DNA. The PCR products of exon 12 in the *c-KIT* from the patients (father and daughter) and 110 healthy volunteers were analyzed by a single strand conformational polymorphism analysis as described [8].

We found that there was a missense substitution at the 5′ first codon of exon 12 (Fig. 2). The G to A mutation at nucleotide position 1775 of the coding region of *c-KIT* resulted in an amino acid substitution from glycine to glutamic acid at position 592 within the intracellular tyrosine kinase domain. The substitution was not present in any of the 110 healthy controls, suggesting that the substitution is not a usual polymorphism but a novel mutation related to piebaldism.

Glycine 592 is conserved among fms family kinases (CSF-1, PDGFR), and is located 4 amino acids upstream from the ATP-binding motif (G-X-G-X-X-G), which is highly conserved among tyrosine kinases [3]. Hypopigmentation due to a L595P mutation located at one amino acid upstream of that motif was reported to be extensive, because L595 was included in ATP binding region [9]. However, the piebald phenotype of the present case was not severe, and G to E conversion of 4 amino acids upstream of G-X-G-X-X-G is also found in *C-SRC* kinase. Therefore 592G might affect activation of fms family kinase receptors regardless of ATP-binding capacity. Therefore G592E mutation may result in loss of function, which phenotype exhibits more mild than that by L595P mutation.

Alternatively, because G1775A is located at the first codon of exon 12 and the mutated allele is ctacagAGAAAA. In this situation, an aberrant splicing can occur as ctacagagAAAA according to the GT–AG splicing rule. This aberrant splicing resulted in a frame sift mutation, and produced nonsense mRNA. Consequently the presented mutation could be consequent to a loss of function.

Piebald patients with pigmental restoration of hypopigmented regions have been investigated in several previous studies, and a mild or modulate phenotype rather than a severe phenotype was observed. In those cases, frame shift mutations in the gene coding for the tyrosine kinase domain of *c*-KIT were identified [4]. It is conceivable that the intracellular frame shifts resulted in loss of function in only half of the c-KIT molecules, resulting in a mild or moderate phenotype.

Melanocytes were considered to exist within the repigmented regions in the present patients and the patients previously reported [4], and the possible existence of melanocytes was formerly investigated within the leukoderma of piebald patients [10]. Furthermore, it has been reported that the repigmented regions were either forehead or knees, which were easily exposed to sunlight [4]. A considerable number of intact c-KIT dimers on the melanocytes within these restricted regions of leukoderma may be required for repigmentation of the piebald patients in the presence of sunlight long after birth. Further investigations will be expected

* *Funding source*: Funded by the grant from the Ministry of Education, Culture, Sports, Science and Technology of Japan and the grant from the Ministry of Health, Labor and Welfare of Japan.

0923-1811/$36.00 © 2011 Japanese Society for Investigative Dermatology. Published by Elsevier Ireland Ltd. All rights reserved.
doi:10.1016/j.jdermsci.2011.08.006

Please cite this article in press as: Arase N, Wataya-Kaneda M. Repigmentation of leukoderma in a piebald patient associated with a novel *c-KIT* gene mutation, G592E, of the tyrosine kinase domain. J Dermatol Sci (2011), doi:10.1016/j.jdermsci.2011.08.006

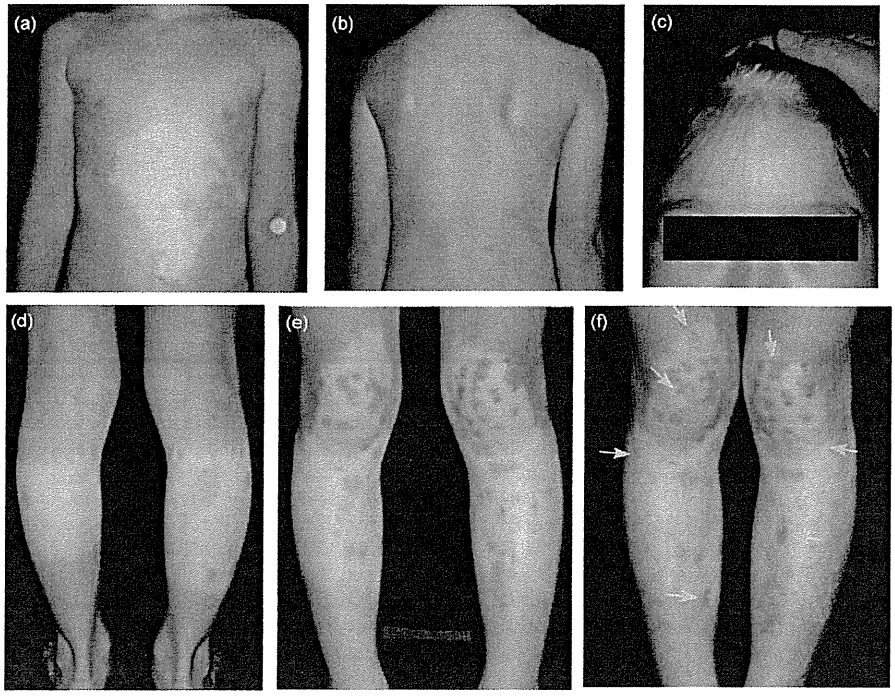

Fig. 1. (a) Leukoderma on the abdomen; (b) small pigmented patches on the back without leukoderma; (c) the white hair on front area of the patient's scalp (white forelock); (d) leukoderma around the popliteal fossas; (e) leukoderma with small pigmented patches around the knees at 5 years of age; (f) several new pigmented patches (indicated with blue arrows) emerged on the leukoderma around the knees at 7 years of age.

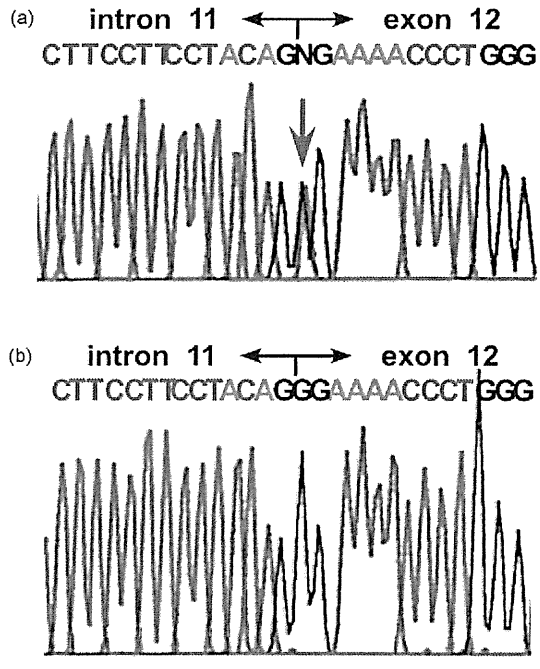

Fig. 2. (a) Genetic analysis of c-*KIT* from the patient revealed a single disease associated heterozygous nucleotide change of 1775 G > A indicated by a red arrow. (b) The single missense mutation was not seen in the analysis of wt DNA.

to clarify the correlation between specific *c-KIT* mutations and pigment regeneration.

References

[1] Giebel LB, Spritz RA. Mutation of the KIT (mast/stem cell growth factor receptor) protooncogene in human piebaldism. Proc Natl Acad Sci U S A 1991;88:8696–9.
[2] Fleischman RA, Saltman DL, Stastny V, Zneimer S. Deletion of the c-kit protooncogene in the human developmental defect piebald trait. Proc Natl Acad Sci U S A 1991;88:10885–9.
[3] Mol CD, Lim KB, Sridhar V, Zou H, Chien EY, Sang BC, et al. Structure of a c-kit product complex reveals the basis for kinase transactivation. J Biol Chem 2003;278:31461–4.
[4] Murakami T, Fukai K, Oiso N, Hosomi N, Kato A, Garganta C, et al. New KIT mutations in patients with piebaldism. J Dermatol Sci 2004;35:29–33.
[5] Narita T, Oiso N, Fukai K, Motokawa T, Hayashi M, Yokoyama K, et al. Two children with a mild or moderate piebaldism phenotype and a father without leukoderma in a family with the same recurrent missense mutation in the kinase domain of KIT. Eur J Dermatol 2011;21:446–7.
[6] Duarte AF, Mota A, Baudrier T, Morais P, Santos A, Cerqueira R, et al. Piebaldism and neurofibromatosis type 1: family report. Dermatol Online J 2010;16:11.
[7] Chong KL, Common JE, Lane EB, Goh BK. A novel mutation in the kinase domain of KIT in an Indian family with a mild piebaldism phenotype. J Dermatol Sci 2010;59:206–9.
[8] Ito S, Suzuki T, Inagaki K, Suzuki N, Kono M, Tomita Y, et al. Two novel mutations detected in Japanese patients with oculocutaneous albinism. J Dermatol Sci 2006;44:116–8.
[9] Lin ZM, Xu Z, Bu DF, Yang Y. New mutations of KIT gene in two Chinese patients with piebaldism. Br J Dermatol 2006;155:1303–4.
[10] Hayashibe K, Mishima Y. Tyrosinase-positive melanocyte distribution and induction of pigmentation in human piebald skin. Arch Dermatol 1988;124:381–6.

Noriko Arase
Mari Wataya-Kaneda*
Department of Dermatology, Osaka University Graduate School of Medicine, 2-2 Yamadaoka, Suita, Osaka 565-0871, Japan

Please cite this article in press as: Arase N, Wataya-Kaneda M. Repigmentation of leukoderma in a piebald patient associated with a novel *c-KIT* gene mutation, G592E, of the tyrosine kinase domain. J Dermatol Sci (2011), doi:10.1016/j.jdermsci.2011.08.006

Naoki Oiso
Department of Dermatology, Kinki University School of Medicine, Osaka, Japan

Atsushi Tanemura
Department of Dermatology, Osaka University Graduate School of Medicine, 2-2 Yamadaoka, Suita, Osaka 565-0871, Japan

Akira Kawada
Department of Dermatology, Kinki University School of Medicine, Osaka, Japan

Tamio Suzuki
Department of Dermatology, Yamagata University School of Medicine, Yamagata, Japan

Ichiro Katayama
Department of Dermatology, Osaka University Graduate School of Medicine, 2-2 Yamadaoka, Suita, Osaka 565-0871, Japan

*Corresponding author. Tel.: +81 6 6879 3031
E-mail address: mkaneda@derma.med.osaka-u.ac.jp
(M. Wataya-Kaneda)

Received 4 April 2011
Revised 17 August 2011
Accepted 21 August 2011

Please cite this article in press as: Arase N, Wataya-Kaneda M. Repigmentation of leukoderma in a piebald patient associated with a novel *c-KIT* gene mutation, G592E, of the tyrosine kinase domain. J Dermatol Sci (2011), doi:10.1016/j.jdermsci.2011.08.006

Case Reports in Dermatology

Case Rep Dermatol 2011;3:107–112
DOI: 10.1159/000328797

Published online:
May 17, 2011

© 2011 S. Karger AG, Basel
ISSN 1662–6567
www.karger.com/cde

This is an Open Access article licensed under the terms of the Creative Commons Attribution-NonCommercial-NoDerivs 3.0 License (www.karger.com/OA-license), applicable to the online version of the article only. Distribution for non-commercial purposes only.

Peculiar Distribution of Tumorous Xanthomas in an Adult Case of Erdheim-Chester Disease Complicated by Atopic Dermatitis

Yukako Murakami[a] Mari Wataya-Kaneda[a] Mika Terao[a]
Hiroaki Azukizawa[a] Hiroyuki Murota[a] Yukiko Nakata[b]
Ichiro Katayama[a]

Departments of [a]Dermatology and [b]Clinical Laboratory Diagnostics, Osaka University Graduate School of Medicine, Osaka, Japan

Key Words
Erdheim-Chester disease · Hand-Schüller-Christian disease · Xanthoma · Atopic dermatitis · Macrophage · CD68 · CD163 · Thymus- and activation-regulated chemokine

Abstract
Erdheim-Chester disease is a rare non-Langerhans form of histiocytosis with multiple organ involvement. Approximately 20% of patients have xanthoma-like lesions, usually on the eyelids. We report a case of Erdheim-Chester disease in a 32-year-old male who showed peculiar xanthomatous skin lesions and also had atopic dermatitis. His skin manifestations included ring-like yellowish tumors on his periorbital regions, rope necklace-like tumors on his neck, and spindle-shaped tumors on his right preauricular region and cubital fossas. He also had exophthalmos and diabetes insipidus. Chronic eczematous lesions were present on the flexor aspect of his extremities, and his serum eosinophil numbers and immunoglobulin E levels were elevated. A histological examination of his right neck tumor showed foamy macrophages and touton-type giant cells, which were positive for CD68 and CD163 and negative for S-100 and CD1a. We suggest that the complication of atopic dermatitis may have contributed to the uncommon clinical features in this case.

Case Report

A 32-year-old male presented with xanthomatous skin lesions, exophthalmos, and diabetes insipidus. His left retro-orbital mass was partially removed in childhood at another hospital, and he had been diagnosed with Hand-Schüller-Christian disease (HSCD). His past medical history included hyperlipidemia, type 2 diabetes mellitus, hypertension, and hyperuricemia, which were managed with

Yukako Murakami, MD

Department of Dermatology
Osaka University Graduate School of Medicine
2-15 Yamadaoka, Suita-City, Osaka 565-0871 (Japan)
Tel. +81 6 6879 3031, E-Mail murakami@derma.med.osaka-u.ac.jp

Case Rep Dermatol 2011;3:107–112
DOI: 10.1159/000328797
Published online: May 17, 2011
© 2011 S. Karger AG, Basel
ISSN 1662–6567
www.karger.com/cde

diet and medication (nateglinide, candesartan cilexetil, and allopurinol). Cutaneous examination revealed ring-like yellowish tumors on his periorbital regions (fig. 1a), rope necklace-like tumors on his neck (fig. 1b, c), and spindle-shaped tumors on his right preauricular region and cubital fossas (fig. 1d). Histological examination of his right neck tumor showed foamy macrophages and touton-type giant cells (fig. 2a). Immunohistochemical staining revealed that the cells were positive for CD68 (fig. 2b) and CD163 (fig. 2c) and negative for S-100 and CD1a. X-rays of the long bones of the upper and lower extremities showed no apparent osteosclerotic or osteolytic changes. Exophthalmos, diabetes insipidus, and the pathological findings confirmed the diagnosis of Erdheim-Chester disease (ECD; table 1). The patient had also been diagnosed with atopic dermatitis in childhood. He demonstrated diffuse facial erythema, pruritic chronic eczematous lesions on the trunk and flexor aspect of the extremities (fig. 1d), and multiple prurigo of the extremities. Laboratory findings related to atopic dermatitis were white blood cells: 12,640/μl, eosinophils: 19%, immunoglobulin E-radioimmunosorbent test (IgE-RIST) score: 38,500 IU/ml, IgE radioallergosorbent test (IgE-RAST) score of *Dermatophagoides farinae*: 99.9 IU, and thymus- and activation-regulated chemokine (TARC): 47,980 pg/ml. Therefore, our patient was diagnosed with ECD complicated by atopic dermatitis.

Discussion

ECD is a rare non-Langerhans form of histiocytosis with multiple organ involvement. Involvement of the long bones is observed in 86% of patients, and a typical manifestation is bilateral symmetric sclerosis of the metaphyseal region of the long bones of the lower extremities [1, 2]. Approximately one half of all cases have extraskeletal manifestations, including effects on the hypothalamus-pituitary axis, lungs, heart, retroperitoneum, skin, liver, kidneys, spleen, and orbit. Skin involvement is seen in approximately 20% of patients, who frequently present with xanthoma-like lesions that usually manifest on the eyelids and occasionally on the trunk and submammary area [3].

Here, we report a case of ECD with a peculiar distribution of tumorous xanthomas and without bone involvement. The patient was initially diagnosed in childhood with HSCD, one of the syndromes of Langerhans cell histiocytosis (LCH), based on the histological findings of his left retro-orbital mass. It is sometimes difficult to distinguish ECD from HSCD because they have certain clinical findings in common such as exophthalmos, diabetes insipidus, and radiological findings of osseous lesions. Osteolysis of the scalp bones is typical in HSCD, whereas osteosclerosis of the long bones is the characteristic presentation of ECD. However, osteosclerosis in ECD is sometimes difficult to identify, and osteolytic lesions are found in approximately one third of patients with ECD [4]. ECD commonly occurs in adulthood, whereas HSCD occurs in infancy. The mortality rate for ECD is 57% and for HSCD it is 30% [5] (table 1).

Immunohistochemical analyses are useful for distinguishing between these two diseases. The histiocytes in the skin involve two major cell lineages, macrophages and Langerhans cells, which are derived from monocytes [6]. Pathogenic macrophages are observed in ECD. In contrast, Langerhans cells are characteristic of HSCD. The histiocytes in ECD are immunoreactive for CD68 and CD163, but not for S-100 or CD1a. The pattern is reversed in histiocytes in HSCD (table 1). Because we were not able to obtain detailed histological information on the left retro-orbital mass removed in childhood, we could not conclude that this was a case of HSCD in childhood that converted to ECD in adulthood, or a case of ECD that showed an HSCD-like manifestation in childhood. Previously, it was suggested but not definitively established that ECD may represent a spectrum of LCH [7, 8]. However, it was recently suggested

KARGER

Case Rep Dermatol 2011;3:107–112
DOI: 10.1159/000328797
Published online: May 17, 2011
© 2011 S. Karger AG, Basel
ISSN 1662–6567
www.karger.com/cde

that ECD is a unique disease entity and LCH-like findings may be within the spectrum of ECD [9, 10]. Further examination of cases and research are needed to explore this issue.

It is interesting that tumorous xanthomas were present mainly in sites predisposed to atopic dermatitis such as the neck skin and flexor aspect of the extremities. Although some cases show nodular xanthomatous masses of the neck [11], rope necklace-like xanthomas and bulging xanthomas on the flexor aspect of the extremities as observed in the present case are rare. We suggest that the complication of atopic dermatitis modified the clinical presentation in this case. Activation of fibroblasts due to scratching behavior evoked by itching due to atopic dermatitis [12] may have resulted in tumorous xanthomas.

In conclusion, we reported a case of ECD with a peculiar distribution of tumorous xanthomas. We suggested that the complication of atopic dermatitis played a role in the development of the uncommon clinical features of our case.

Table 1. Hand-Schüller-Christian disease and Erdheim-Chester disease

	Onset	Clinical sign	Mortality	Proliferated histiocyte	S-100	CD1a	CD68	CD163
HSCD	Infant	DI, exophthalmos, osteolysis of the scalp bone	30%	Langerhans cell	+	+	–	–
ECD	Adult	DI, exophthalmos, osteosclerosis of long bones (sometimes osteolysis)	57%	Macrophage	–	–	+	+

DI = Diabetes insipidus; HSCD = Hand-Schüller-Christian disease; ECD = Erdheim-Chester disease.

KARGER

Case Reports in Dermatology
Case Rep Dermatol 2011;3:107–112
DOI: 10.1159/000328797
Published online: May 17, 2011
© 2011 S. Karger AG, Basel
ISSN 1662–6567
www.karger.com/cde

Fig. 1. **a** Ring-like yellowish tumors in the periorbital regions. **b**, **c** Rope necklace-like yellowish tumors on the patient's neck. **d** Spindle-shaped yellowish tumors on the patient's cubital fossas and diffuse erythema and pigmentation on the patient's forearm.

KARGER